AIAA/AAS Astrodynamics Specialist Conference and Exhibit
18 - 21 August 2008, Honolulu, Hawaii

AIAA 2008-6450

Passive Vertical Stabilization of Two Tethered Nanosatellites with Engineered Damping

Nicolas N. Lee* and Alan H. Zorn*
Stanford University, Stanford, CA 94305

Matthew West†
University of Illinois, Urbana, IL 61801

A simple method for the vertical stabilization of two tethered nanosatellites in low Earth orbit is described. Without active attitude control or passive damping, the satellite system would freely oscillate like a pendulum due to the gravity gradient moment acting differentially on the displaced satellites. It would also vibrate axially like a bouncing ball as the tether cycles from tautness to slackness. What ambient friction exists within the satellite system might eventually damp out these librations and vibrations, but with small space structures such dissipative mechanisms are meager: undesirable oscillations could persist for months.

The performance benefit of engineering a passive spring-damper mechanism along the length of the tether connecting the two nanosatellites is investigated. Two-dimensional orbital-plane analysis only is given in this paper. The axial spring-damper is tuned by frequency matching the axial and in-plane librational modes so that they are coupled as strongly as possible. The coupling encourages the two modes to exchange energies. Over time, net energy is removed from the librations and dissipated by the axial spring-damper mechanism. The system is driven towards stable equilibrium. It is shown that a stiff spring is inadequate; there must be significant play in the tether when it is in tension for the scheme to work. The tuned parameters are shown to perform well over a broad range of initial conditions, from deployment to near stable equilibrium. Except when initialized near the unstable equilibrium, the method reduces the amplitude of in-plane librations by a factor of five in about one day for most initial conditions. The axial vibrations are seen to attenuate in unison with the librations.

I. Introduction

The space tether has long been envisioned as a means for spacecraft formation flying, vertical attitude stabilization, orbit modification, and electrical power generation. First envisioned in the late nineteenth century, the idea of tethering satellites together gained momentum in the 1960's and 1970's. Space tether mission concepts arose that included applications in antenna pointing, tether propulsion and electrodynamic-powered tethers.

In 1992, NASA jointly with the Italian Space Agency delivered the Tethered Satellite System-1 (TSS-1) to Earth orbit.[1] Space Shuttle Atlantis reeled out a 515 kg satellite on a tether of length 260 m. Practical approaches to tether deployment, control and retrieval were tested on this mission, and theoretical analysis of the dynamics of space tethers was demonstrated in space. With various degrees of success, subsequent tether missions were conducted by NASA/Italian Space Agency and later by the European Space Agency. In these later missions, the tethers were of lengths 20 to 30 km and the tethered satellite mass ranged from 36 to 500 kg. In 1996, the Tether Physics and Survivability (TiPS) satellite was launched by the Naval Center for Space Technology. This satellite demonstrated gravity-gradient stabilization using a 4 km tether. Observations of this satellite indicated that librational oscillations damped from an amplitude of 40° to 5° over a period of seven months.[2] More recently, the Multi-Application Survivable Tether (MAST) nanosatellite was built by

*Ph.D. Candidate, Department of Aeronautics and Astronautics, Durand Building, 496 Lomita Mall, Stanford, CA 94305, Student Member AIAA.

†Assistant Professor, Department of Mechanical Science and Engineering, 158 MEB, M/C 244, Urbana, IL 61801, Member AIAA.

Copyright © 2008 by the American Institute of Aeronautics and Astronautics, Inc. All rights reserved.

Tethers Unlimited, Inc. and Stanford University and launched in 2007.[3] The 1 km tether, however, failed to fully deploy.

At Stanford University's Space Systems Development Laboratory (SSDL), our primary mission is to enable nanosatellites to achieve more relevant scientific missions with minimal increase in complexity. One area where nanosatellites have room for improvement is attitude control. Recent missions have relied on passive magnetic stabilization to maintain alignment with the Earth's magnetic field, but this forces the satellite to tumble at twice the orbital rate. For many missions, a nadir-pointing satellite is a requirement, either for a scientific payload to study the Earth or for a directional antenna to achieve the necessary bandwidth for communication. A tethered pair of nanosatellites could be deployed so that a vertical orientation is maintained with respect to the Earth by means of gravity gradient stabilization.[4]

Tethered systems librate freely in orbit, as would any object possessing a nonspherical moment of inertia.[5] Long transients may persist in reaching vertical stabilization unless some means of damping is provided. Damping is easily mechanized along the length of the tether, in the axial direction between the two nanosatellites. But axial damping does not normally damp out librations; some means are required to damp out librations in a reasonable amount of time.

Gravity gradient stabilization has successfully been used on much larger and more massive conventional satellites in Earth orbit. In larger satellite systems, internal effects such as fuel sloshing, flexing of booms, or thermal expansion and contraction may be sources of passive damping. But there is not much opportunity for such ambient damping to exist in a nanosatellite, thus there is more of a need to engineer the damping into a tethered nanosatellite system.

Conventional satellites are typically rigid bodies, whereas tethered nanosatellites are not. There are, however, several similarities. Because of the natural centripetal force constantly forcing the two apart, the tethered satellites when near librational and axial equilibrium maintain tautness in the tether, thus acting much like a rigid body. Also when near the stable equilbrium, the equations of motion depend little on mass or tether length: the dynamical motion, natural frequencies and energy exchanges are nearly the same. Despite these similarities, nanosatellites have much smaller mass than conventional satellites, so are more susceptable to external disturbances.

Early in the investigation, two possible damping mechanisms were identified:

- Axial mechanism: the tether itself acts as a spring-damper in the axial direction; and
- Rotational mechanism: a rotational spring-damper is implemented at the anchor points where the tether connects to the nanosatellites.

The axial mechanism is inherent in the tether system, but is only weakly coupled with in-plane librations and not coupled at all with out-of-plane librations. The rotational mechanism adds additional damping which is more strongly coupled to both types of librational oscillations, but is more complex to implement. Further analysis suggested that a design with only axial damping works quite well to stabilize in-plane librations, avoiding the complexity of the rotational mechanism. It is this design we report on here.

In this paper, the following solution to the tethered nanosatellite stabilization problem is proposed:

- A simple spring-damper mechanism is engineered into the tether;
- The spring-damper is tuned to frequency match the axial and in-plane librational dynamics;
- Librational energy is transferred to axial energy which is then dissipated by the spring-damper mechanism.

The spring-damper could be engineered into the tether material or as a mechanism attached to the tether. Alternatively, the damping could be built into a reel that controls the extent of the tether. As the tether reels out, friction in the reel would remove mechanical energy from the two-satellite system. The precise nature of the spring-damper mechanism is not of interest in this paper; rather we focus on characterizing the spring and damping properties that would be required to provide satisfactory stabilization.

We show that a simple and lightweight tether constructed as such would enable two nanosatellites to become passively oriented with respect to vertical in the orbital plane within a day or two after deployment. There would be no need for active attitude control. The nanosatellites would be capable of undertaking Earth-observation missions while ensuring that cameras, scientific instruments, and communication antennae are nadir-pointing.

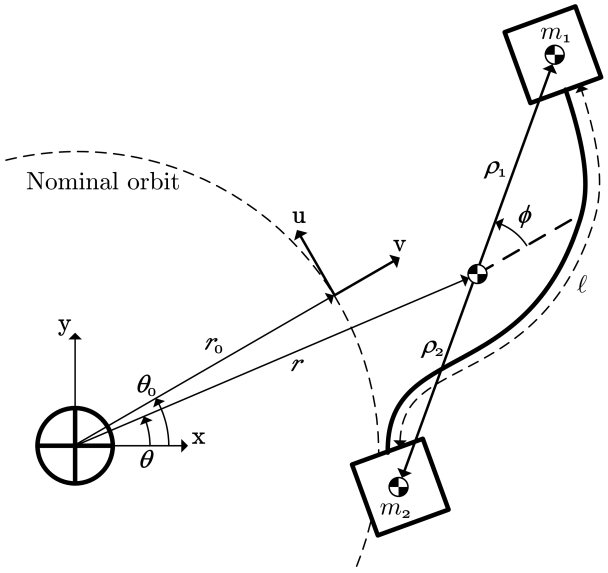

Figure 1. The Earth-Centered Inertial and Local Level coordinate frames are depicted, with two tethered nanosatellites orbiting. The tether length is l.

It is anticipated that deployment is initiated by a simple spring mechanism. No other deployment control is envisioned other than that provided naturally by the gravity gradient. It is thus important to characterize performance of our scheme under a wide range of initial conditions. Since small satellites are more prone to external disturbances, it is also important to characterize performance under a wide range of disturbance impulses. It is desireable for stable equilibrium to be reached as quickly as possible after deployment, and after a disturbance impulse. Results are presented in both of these situations.

The paper is organized as follows. Section II provides definitions and conventions for the development of the equations of motion presented in Section III. Section IV then illustrates the design visually by simulating the system under various conditions. This section also provides a discussion on tuning the spring-damper mechanism in terms of classic control design principles. Analysis of energy is provided in Section V, where a Lyapunov function is proposed to certify stability over a wide range of initial conditions.

II. Nomenclature

The nominal orbit of the tethered nanosatellite system is defined as that of the center of mass placed in a circular orbit at a desired orbital radius, r_0, when the tether length is in axial equilibrium and the two masses are in stable librational equilibrium. Under these conditions, the tether is stretched to exactly balance centripetal force and the two masses are aligned vertically in librational (gravity gradient) equilibrium. Since the system is in a circular orbit, the nominal mean motion ω_0 is constant. The nominal true anomaly is then

$$\theta_0(t) = \omega_0(t - t_0) \tag{1}$$

where t_0 is the epoch.

Two coordinate frames are illustrated in Fig. 1. They are defined as follows:

- Earth-Centered Inertial (x-y-z). The x-y plane is the orbital plane; z is in the direction of the angular momentum vector.
- Local Level (v-u-w). The local level frame is the same as the x-y-z frame at time of epoch, except that the origin of the local level frame is at the nominal center of mass. The coordinate directions u and v lie in the orbital plane: u is in the direction of forward orbital motion (along track) while v is vertical. The coordinate w is in the same direction as z. The local level frame rotates about the w axis at the constant rate of the nominal mean motion ω_0.

A list of parameters and variables used in this paper are as follows:

Physical quantities:

μ	Earth's gravitational constant (3.986004418 x 10^{14} m^3/s^2)
r_e	Earth's equatorial radius (6,378,137 m)
h	Altitude of circular orbit, m
m	Mass intensity at each end of tether, kg
M	Total system mass, kg ($M = 2m$)
k	Tether spring constant, N/m
b	Tether damping constant, N/(m/s)
ℓ	Free length of tether, m
L	Maximum length of tether, m (satellite scale)
ρ_0	Half-length of tether when system is in stable equilibrium, m
r, r_0	Actual, nominal distance of center of mass from center of Earth, m
θ, θ_0	Actual, nominal true anomaly of center of mass, rad
g, g_0	Actual, nominal magnitude of local gravity, m/s^2
ω, ω_0	Actual, nominal mean motion, rad
ξ, ξ_0	Actual, nominal scale ratio ($2\rho/r$, $2\rho_0/r_0$)

Simulation parameters:

T	Simulation time

Phase variables:

u	Along-track displacement from nominal orbit, m
v	Vertical displacement from nominal orbit, m
ρ	Half-distance between tethered satellites, m (the vectors $\rho = \rho_1 = -\rho_2$ in Fig. 1)
ϕ	Libration angle referenced to vertical, rad
$\dot{u}$	Along-track component of velocity relative to rotating nominal frame, m/s
$\dot{v}$	Vertical component of velocity relative to rotating nominal frame, m/s
$\dot{\rho}$	Rate of change of half-distance between tethered satellites, m/s
$\dot{\phi}$	Libration angular rate, rad/s

Energy and power:

e	Total specific energy, J/kg
p	Specific dissipation power, W/kg

III. Equations of Motion

We now define the problem, state the assumptions that lead to the equations of motion, and proceed to develop the equations of motion.

Consider the motion of two equal point masses tethered together orbiting a point mass Earth. The motion of each mass is restricted to the orbital plane. Out-of-plane librations are not considered herein, but are an important consideration. The tether is assumed to be massless and is represented mathematically by an axial tension along the line that joins the two masses. When the tether is taut, the tension is given by a linear spring-damper with spring constant k and damping constant b. When slack, there is no force between the two bodies. The axial force is thus nonlinear. The spring-damper could be designed with active components or with time-varying or nonlinear coefficients, but for this investigation we focus on the simplicity of constant coefficients.

Prior to deployment, the two nanosatellites are in their launch pod almost touching each other, with the tether slack. At deployment, a spring mechanism forces them and the tether out of the pod. The nanosatellites will separate because of slightly differences in initial velocities. They are in slightly different orbits, hence will drift apart until they reach the tether limit. Were no damping applied, the satellites would rebound elastically as the tether becomes taut. They would then continue to rebound within the constraints of the tether in a somewhat chaotic manner. When damping is applied, however, they tend to align vertically after some time. The tether is constantly kept in tension by the tendency of the satellites to drift apart (centripetal force), resulting in a system which is equivalent to a rigid dumbbell. This results in the gravity

gradient stabilization of the nanosatellite pair.

Expressions for the gravitational force and moment that act on the tethered nanosatellite system are first developed. An approximation is used in these expressions, and justification is offered. Three modes will be seen to describe the tethered system:

- The *orbital dynamics* describe the motion of the center of mass of the tethered nanosatellite system. Two nonlinear second-order differential equations result from applying Newton's Second Law to the linear motion of the center of mass, as it is influenced by the gravitational force. The gravitational force is the only external force acting on the system.
- The (in-plane) *librational dynamics* govern the oscillation of the axial line that intersects the two masses about their center of mass. One nonlinear second-order differential equation results from applying Newton's Second Law to the angular motion of the tethered nanosatellite about the center of mass, as it is influence by the gravitational moment. The gravitational moment is the only external moment acting on the system.
- The *axial dynamics* reflect the displacement between the two masses in the axial direction (along the line that intersects the two masses). The axial dynamics implement the spring/mass mechanism engineered into the tether, and result in one nonlinear second-order differential equation.

Corresponding to each second-order differential equation is a configuration variable and a momentum variable, resulting in eight phase variables for the two-dimensional analysis.

A. Assumptions

We consider the motion of two nanosatellites tethered together in low Earth orbit. The following assumptions are made:

1. The Earth is a point mass that is fixed inertially. In particular, non-inertial motion of the Earth about the Sun is ignored.
2. There are no other external disturbing forces.
3. The tether is massless, has no bending stiffness, and cannot be tangled.
4. The nanosatellites have equal mass m. The system mass is thus $M = 2m$.
5. The tether is connected to the nanosatellites at their center of mass.
6. The moments of inertia of the nanosatellites are spherically symmetric.
7. The motion of each tethered mass is restricted to the two-dimensional orbital plane.
8. The initial orbit of the center of mass is circular at a distance r_0 from the center of the Earth.
9. The tether and the two masses can be enclosed in a sphere of diameter L at all times.
10. The ratio L/r_0 is small.

Assumptions 5 and 6 allow us to model the nanosatellites as point masses. The parameter L is sometimes called the satellite scale. Soon we shall see that L in relation to r_0 governs the quality of an approximation made to allow tractable mathematical representation of the gravitational force and moment acting on the satellite system.

B. Gravitational Force

The gravitational force acting on an orbiting system of particles is given by[6]

$$\mathbf{F} = \mathbf{F_g} + \mathbf{F_{gg}} = -\frac{\mu M}{r^2}\hat{\mathbf{v}} + \frac{\mu}{r^4}\left\{\frac{15}{2}\left(\hat{\mathbf{v}}^{\mathrm{T}}\mathbf{I_c}\hat{\mathbf{v}}\right)\hat{\mathbf{v}} - \frac{3}{2}\left(\mathrm{tr}\ \mathbf{I_c}\right)\hat{\mathbf{v}} - 3\mathbf{I_c}\hat{\mathbf{v}}\right\} \tag{2}$$

where r is the distance of the center of mass from the center of Earth, $\hat{\mathbf{v}}$ is the unit vector in the vertical direction, M is the total mass of the system, and $\mathbf{I_c}$ is the moment of inertia about the center of mass. The system of particles need not be a rigid body, such as when a tether goes slack, thus $\mathbf{I_c}$ is generally time-varying.

The first term $\mathbf{F_g}$ in Eq. (2) is easily recognized as the inverse square law which acts on the center of mass as if the total mass were concentrated there. The second term $\mathbf{F_{gg}}$ is the gravity gradient force. Note that when the moment of inertia does not represent a spherically symmetric body, such as for a tethered satellite system, $\mathbf{F_{gg}}$ may have a non-central component as well as a central component. In any case, the gravity gradient force is very small. For a tethered satellite orbiting at 800 km with a 5 m tether, the magnitude of the specific force $\mathbf{F_{gg}}/\mathbf{M}$ does not exceed 2×10^{-11} m/s^2. *That's 2 pico-g's.* The term is routinely dropped when satellite motion is being computed; it has negligible effect on the trajectory. It is crucially important, however, to carry this term when analyzing energy and angular momentum. Without it, conservation is totally lost and false conclusions can be made about energy and angular momentum exchange.

When parameters specific to the problem at hand are substituted in, reduced to two dimensions, and scaled by the total mass M to represent specific force, Eq. (2) becomes

$$f_u = -g\sin(\theta - \theta_0) + g\xi^2\left\{\frac{3}{8}(5\sin^2\phi - 2)\sin(\theta - \theta_0) + \frac{3}{4}\sin\phi\cos(\theta - \theta_0 + \phi)\right\} \tag{3}$$

$$f_v = -g\cos(\theta - \theta_0) + g\xi^2\left\{\frac{3}{8}(5\sin^2\phi - 2)\cos(\theta - \theta_0) + \frac{3}{4}\sin\phi\sin(\theta - \theta_0 + \phi)\right\} \tag{4}$$

where $g = \mu/r^2$ is the local value of gravity, $\xi = 2\rho/r$ is the scale ratio, and ρ is the half-distance between the nanosatellites. The scale ratio ξ is on the order of 10^{-6} for the tethered nanosatellite system, so the smallness of $\mathbf{F_{gg}}$ in Eq. (2) is clearly revealed in Eqs. (3) and (4).

The appendix provides algebraic relationships which when substituted into Eqs. (3) and (4) express them completely in terms of the configuration variables u, v, ρ and ϕ.

C. Gravitational Moment

The gravitational moment can be derived from Eq. (2) as

$$\mathbf{M_c} = \mathbf{F} \times \mathbf{r} = -3\frac{\mu}{r^3}\ \mathbf{I_c}\hat{\mathbf{v}} \times \hat{\mathbf{v}} \tag{5}$$

where $\mathbf{M_c}$ is the gravitational moment acting on the system of particles about its center of mass and $\mathbf{r} = r\hat{\mathbf{v}}$. Again, the system of particles need not be a rigid body. This moment is the primary driver of librational motion.

When parameters specific to the problem are substituted in, reduced to two dimensions, and scaled by the total mass M to represent specific moment, Eq. (5) becomes

$$m_c = -3\omega^2\rho^2\frac{\sin 2\phi}{2} \tag{6}$$

where $\omega^2 = \mu/r^3$ and m_c is now a scalar that gives the specific moment about the z axis.

D. Justification of Approximation

Equations (2) and (5) are approximations to the true gravitational force and moment, hence so are Eqs. (3), (4) and (6). They are Taylor series expansions about $\xi = 2\rho/r_0$ to second order. Thus for any orbiting system of particles, the approximation is good to $\mathrm{O}(\xi^3)$. Due to symmetries present in the geometry of tethered nanosatellites, the approximation is actually good to $\mathrm{O}(\xi^4)$ for Eqs. (3), (4) and (6). For example, $\xi \approx 10^{-6}$ for a 5 m tether, which means the approximation to specific force is good to about $10^{-24}g$. A

yocto-g is a pretty small specific force, thus one would naturally expect that dropping the $O(\xi^4)$ terms would be appropriate.

But danger lurks in every approximation. For example, one would also expect that ignoring the $O(\xi^2)$ term in Eqs. (3) and (4) would also be a valid aproximation, which as pointed out in Subsection B corresponds to pico-g's of error. Our investigation has shown that ignoring the $O(\xi^2)$ terms is a very good approximation to the specific force when studying phase-space motion. But we also found that without the term, the resulting dynamics fail miserably to portray enchanges of energy or angular momentum. Conservation of angular momentum is completely lost, and even when no damping is in place, conservation of energy disappears completely. The result would be a catestrophically incorrect assessment of angular momentum and energy exchange. Besides, if the $O(\xi^2)$ term were ignored in Eq. (6), the moment equation, there would be no librations.

We return to the argument of ignoring the $O(\xi^4)$ terms. To the numerical precision of our computers, simulations show there is no difference in results between ignoring the $O(\xi^4)$ terms and using exact analytic expressions.

E. Orbital Equations of Motion

We now apply Newton's Second Law to the external forces given in Eqs. (3) and (4). The kinematics of the center of mass of the tethered nanosatellite system are easily transformed into the rotating nominal local level frame, resulting in

$$\ddot{u} + 2\omega_0 \dot{v} - \omega_0^2 u = f_u \tag{7}$$

$$\ddot{v} - 2\omega_0 \dot{u} - \omega_0^2 v = f_v + g_0. \tag{8}$$

The orbital dynamics are seen to be linear to inputs of specific force, f_u and f_v. The natural frequency of the response is at the orbital rate; for example, an 800 km circular orbit has an orbital period of about 100 minutes. This oscillation is induced by Coriolis exchange between u and v. There are also two poles at the origin associated with the irrelevance of initial true anomaly. This is a defective[a] double pole: it is represented by only one eigenvector aligned in the horizontal **u** direction. True anomaly can arbitarily be translated without affecting the motion of the system, and this is the only phase variable or linear combination to which this statement applies.

F. Librational Equation of Motion

The specific angular momentum about the center of mass can be expressed as

$$h_c = \rho^2 \left(\dot{\theta} + \dot{\phi} \right). \tag{9}$$

We now apply Newton's Second Law for moments:

$$\dot{h}_c = m_c \tag{10}$$

where m_c is found in Eq. (6). This results in

$$\frac{d}{dt} \left\{ \rho^2 \left(\dot{\theta} + \dot{\phi} \right) \right\} = -3\,\omega^2 \rho^2 \frac{\sin 2\phi}{2} \tag{11}$$

where $\omega^2 = \mu / r^3$. Differentiating and rearranging terms results in the equation of motion for librations:

$$\ddot{\phi} + 3\omega^2 \frac{\sin 2\phi}{2} = -\ddot{\theta} - \left(\frac{2\dot{\rho}}{\rho} \right) \left(\dot{\theta} + \dot{\phi} \right). \tag{12}$$

The appendix contains algebraic relationships which when substituted into Eq. (12) express it completely in terms of the phase variables.

Near the stable equilibrium, the natural libration frequency is $\sqrt{3}\,\omega$. Thus for a 100-minute orbit, the libration period is 58 minutes.

[a]Recall from linear algebra that a *defective matrix* is one that does not have a full set of eigenvectors.

A deliberately detailed development of the librational equations of motion was presented in order to make the following observations. Referring to Eqs. (11) and (12), one can see that without variation in ρ there can be no direct exchange of energy between the librational and axial dynamics. Thus when axial motions are small, as when a stiff spring is used, they are barred from significantly influencing librations. There must be significant play in the tether when it is in tension for the desired energy exchange to take place. Furthermore, as we shall see in Section IV, damping axial motion too rapidly or too slowly also results in little energy exchange. These two observations suggest that librational dissipation can take place only when tuning of the spring constant k and the damping constant b is properly coordinated.

G. Axial Equation of Motion

The axial dynamics reflect the relative displacement of the two masses. A rigid dumbbell satellite would have no such dynamics; the length would be fixed. A tether can be slack or taut, hence we promote this length constant to a configuration variable, allowing the distance between the two nanosatellites to vary. It is more convenient to use the half-distance between the two point masses, ρ, as the configuration variable. The half-distance ρ also represents the the distance between either mass and the center of mass at any given time.

We model the spring-damper mechanism built into the tether as follows. When slack, there is no internal force between the two masses; when taut, a linear spring-damper is active allowing the tether to stretch beyond its free length. The axial dynamics are then given by

$$\ddot{\rho} + \left\{ \frac{b}{m}\dot{\rho} + \frac{k}{m}\left(\rho - \frac{\ell}{2}\right) \right\}_+ = \rho\left(\dot{\theta} + \dot{\phi}\right)^2 + g\xi\frac{3\cos^2\phi - 1}{2} - g\xi^3\frac{15\cos^2\phi - 3}{16} \tag{13}$$

where $\{\cdot\}_+$ is equal to the enclosed expression when the tether is taut ($\rho \geq \ell/2$) and equal to zero when slack. The first term on the right-hand side can be recognized as the centripetal (specific) force that tends to force the tether taut. The last two terms adjust for the gravity gradient force differential in the axial direction (this is a tension gradient, to be distinguished from the torsion gradient that induces the librational motion). The final of these two terms can be neglected, but is retained here for completeness.

Again, the appendix contains algebraic relationships which when substituted into Eq. (13) express it completely in terms of the phase variables.

H. Equilibrium Conditions

With a tether or rigid dumbbell, there is only one stable equilibrium configuration: the nanosatellites fly in vertical formation. But there is also an unstable equilibrium in which they they fly in horizontal formation. We are not too interested in this unstable equilibrium, but point out that when initial conditions are near the instability, settling times will extend considerably. All eight phase variables must be just right for this to happen, so we will not examine this case in too much detail.

The nominal values of the phase variables corresponding to the system in stable equilibrium are

$$u_0 = 0 \qquad \dot{u}_0 = 0 \tag{14}$$

$$v_0 = 0 \qquad \dot{v}_0 = 0 \tag{15}$$

$$\phi_0 = 0 \qquad \dot{\phi}_0 = 0 \tag{16}$$

$$\rho_0 = \left(\frac{\frac{k}{m}}{\frac{k}{m} - 3\omega_0^2}\right)\frac{\ell}{2} \qquad \dot{\rho}_0 = 0. \tag{17}$$

The nominal system is in a circular orbit, so has constant mean motion which can be shown to be

$$\omega_0 = \sqrt{\left(\frac{1 + (\frac{\rho_0}{r_0})^2}{(1 - (\frac{\rho_0}{r_0})^2)^2}\right)\left(\frac{\mu}{r_0^3}\right)}. \tag{18}$$

This is almost negligibly different than the mean motion that would be experienced were all the mass concentrated at the center of mass, orbiting in Keplerian fashion. The mean motion of Eq. (18) is a bit faster, since the lower mass dips into the gravitational well slightly more than the upper mass sticks out.

Given μ, r_0, k, m and ℓ, Eqs. (17) and (18) can be iterated to yield ρ_0 and ω_0 (two iterations starting with $\rho_0 = 0$ will do it). When $k/m \leq 3\omega_0^2$, a stable equilibrium does not exist. We ensure a stable equilibrium is reachable by setting k sufficiently large that this condition does not occur.

I. Linearized Equations of Motion

The nonlinear dynamics are given by Eqs. (7), (8), (12) and (13). Linearizing them about the stable equilibrium results in:

$$\ddot{u} + 2\omega_0\dot{v} - \frac{3}{4}\omega_0^2\xi_0^2 r_0\phi = 0 \tag{19}$$

$$\ddot{v} - 2\omega_0\dot{u} - 3\omega_0^2 v + 3\omega_0^2\xi_0\delta\rho = 0 \tag{20}$$

$$\delta\ddot{\rho} + \frac{b}{m}\delta\dot{\rho} + \left(\frac{k}{m} - 3\omega_0^2\right)\delta\rho - \omega_0\xi_0 r_0\dot{\phi} - \omega_0\xi_0\dot{u} + 3\omega_0^2\xi_0 v = 0 \tag{21}$$

$$\ddot{\phi} + 3\omega_0^2\phi - \frac{2\omega_0}{r_0}\dot{v} + \frac{2\omega_0}{\rho_0}\delta\dot{\rho} = 0. \tag{22}$$

Note that r_0 is the only independently selectable parameter and $\xi_0 = 2\rho_0/r_0$ is the derived nominal scale ratio. The coupling between the equations is illustrated in Fig. 2.

Several observations can be made:

- The poles associated with the orbital dynamics (0, 0, $j\omega_0$, $-j\omega_0$) are effectively immovable by the spring constant k and damping constant b. The system is stuck orbiting at its nominal rate.
- The librational poles are very near $\pm j\sqrt{3}\,\omega_0$ for all k and b. They do, however, wander into the left-half plane a little as the spring and damping constants are varied. But as mentioned in Subsection F, there must be variation in $\dot{\rho}$ for this to happen: significant and relatively slow action in the axial dynamics is the only way to influence librations.
- When the tether is completely stiff, it is a dumbbell satellite and ρ is constant. In this situation, it would appear that there is negligible coupling of librations into orbital motion since ξ_0^2 is small. In fact, the term in Eq. (19) that contains ξ_0^2 can safely be ignored for motion simulation. The librational and orbital dynamics completely decouple in this case.
- It is most important *not* to ignore the term in Eq. (19) that contains ξ_0^2 when evaluating energy and angular momentum exchanges, whether the tether is stiff or not. The reason for this is explained more fully in Section V.

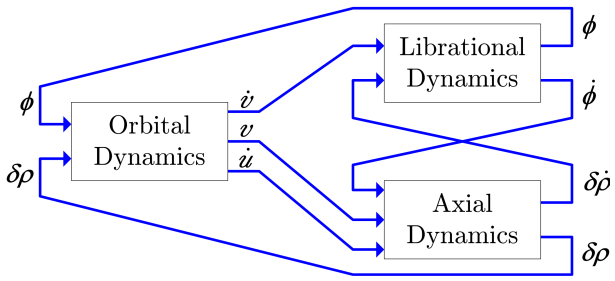

Figure 2. The four linearized equations of motion result in oscillatory dynamics in the orbital, librational, and axial modes. The orbital dynamics depend only on configuration variables. The librational and axial dynamics are cross-coupled only with momentum (rate) variables. It is through this rate coupling that librations are damped out.

IV. Simulation Results

The motion of the tethered nanosatellites was simulated with various spring and damping constants and under various initial conditions. Both the linear and nonlinear equations of motion were implemented. The linear system was used to select the tether spring and damping constants for good performance, and to simulate the system response to small perturbations from stable equilibrium. The nonlinear system was used to simulate scenarios with large deviations from equilibrium, such as during deployment. The two simulations were verified against each other when initialized to near-equilibrium conditions.

Our results focus on the transient response due only to initial conditions, and not to a continuously applied disturbance. Studying the transient response due to an initial condition is equivalent to that of imposing a continuous disturbance, then turning the disturbance off (impulsive disturbance).

A. Simulation Conditions

Baseline simulation conditions are chosen to be representative of a typical nanosatellite mission:

$$h = 800 \text{ km} \tag{23}$$

$$m = 1 \text{ kg} \Rightarrow M = 2 \text{ kg} \tag{24}$$

$$\ell = 5 \text{ m}. \tag{25}$$

The altitude is high enough that atmospheric drag will not signficantly disturb a small satellite system. For any space structure of a given density, the ratio of cross-sectional area to mass is inversely proportional to satellite scale. A small satellite system is thus influenced more by atmospheric drag than a large system, hence the choice of a higher than normal altitude. The other two parameters are merely representative. Tuning the spring and damping constants is not very sensitive to the choice of satellite mass or tether length.

B. Performance Tuning

The linear simulation is used to tune the spring and damping constants for good transient performance. Given a spring constant k, frequency-domain techniques are used to select a damping constant b that results in the quickest damping of librations. In the left plot of Fig. 3, a root locus of the system poles is shown for a spring constant of 0.0001 N/m as the damping constant is varied.

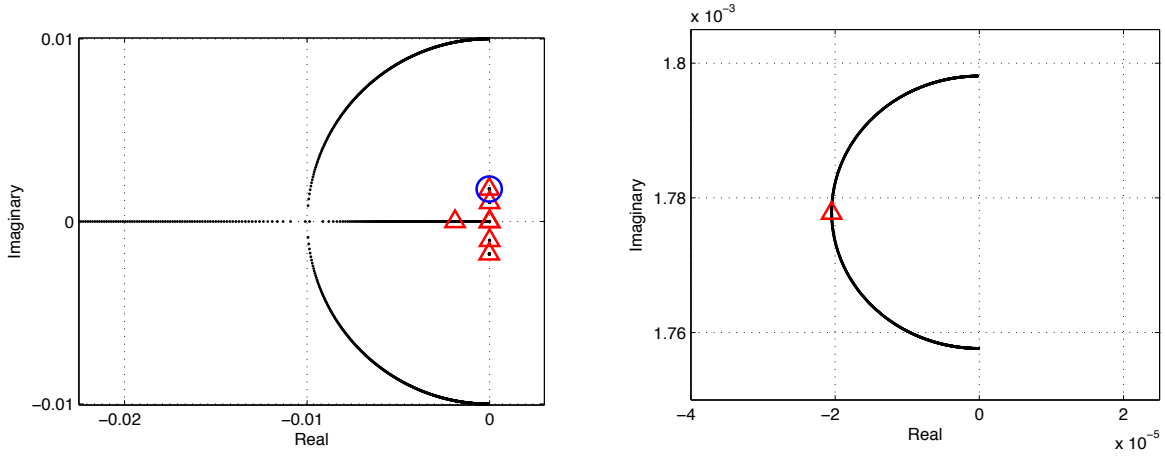

Figure 3. The system poles trace out a locus as the damping constant b is varied. Two orbital poles are at the origin and another two are on the imaginary axis. Further up the imaginary axis are the two librational poles. The upper one is circled in blue. The axial poles trace out the large semicircle which diverges to two poles on the negative real axis. The upper librational pole is shown in more detail on the right. It also traces out a semicircle. The damping constant is selected to maximize the negative real part of this pole. The red triangles denote the system poles for the selected damping constant.

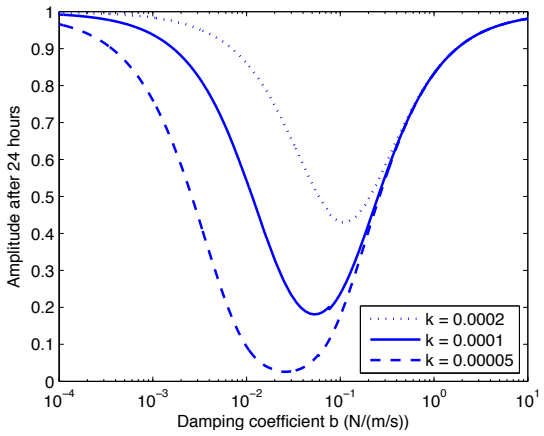

Figure 4. For three spring constants and a range of damping constants, the linear system is simulated for 24 hours. The ratio of the final to initial librational amplitude is plotted as a function of the damping constant. The minima indicate the damping constants which achieve maximum librational damping. Stiffer springs are less able to damp out librational oscillations.

The right plot of Fig. 3 zooms in on the upper librational pole tracing out a semicircle. The damping constant b is selected so that this pole is as far into the left-half plane as possible. It is worth noting that when the librational pole is driven as far into the left-half plane as possible, one of the axial poles matches the frequency of the librational mode. The resulting resonance between the two modes enables the fastest energy transfer out of the librational mode into the axial mode where it is dissipated.

Figure 4 shows the librational amplitude after 24 hours for three different spring constants and a range of damping constants. The amplitude is normalized to the initial librational amplitude. As the spring constant loosens, the optimal damping constant decreases while the librational dissipation rate increases.

Figure 5 illustrates the best possible system performance for a range of spring constants. Figure 6 shows that maximum damping results when this relationship is linear: $b \approx (540 \text{ s})\ k$.

In general, it appears that it is preferable to have as loose a spring as possible given practical constraints on material properties and maximum allowable tether stretch. Once a spring constant is chosen, the damping constant can be computed. For the following discussion on system response, a spring constant of 0.0001 N/m is selected to obtain a reasonable settling time, and a damping constant of 0.054 N/(m/s) is selected to maximize the rate of librational damping.

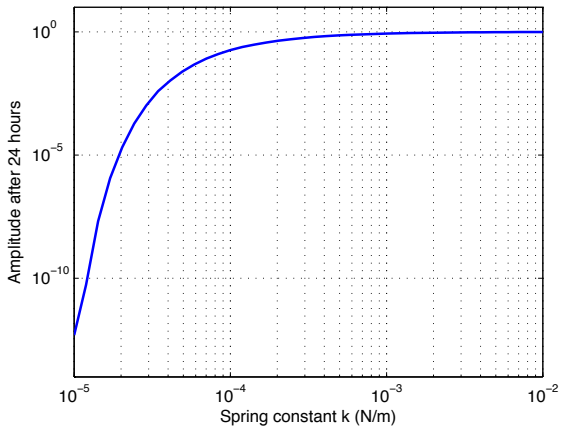

Figure 5. The minimum librational amplitude after 24 hours is plotted as a function of spring constant. Looser springs are more able to damp librational oscillations quickly.

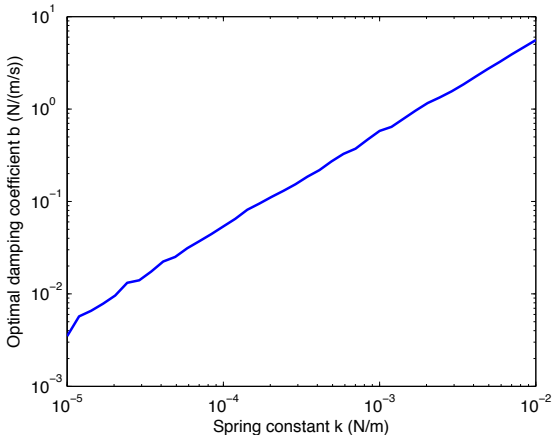

Figure 6. The optimal damping constant is plotted as a function of spring constant. The relationship is approximately linear with a proportionality constant of 540 s.

C. Linear Response

When the system is near the stable equilibrium, the linearized equations of motion faithfully approximate the nonlinear equations. With the system coefficients chosen above, small perturbations to the initial conditions are applied to verify that the system behaves as the pole-zero map indicates. A selected example is presented with the following initial conditions:

$$\phi(0) = 20^\circ \qquad \dot{\phi}(0) = 0 \tag{26}$$

$$\rho(0) = \rho_0 + 0.05 \text{ m} \qquad \dot{\rho}(0) = 0. \tag{27}$$

The time-history of ϕ and ρ for a two-day period is shown in Fig. 7. The tether is axially overdamped, but is coupled to the librational oscillations. The oscillations damp out exponentially as expected since the librational poles have been moved to the left-half plane.

A wide variety of initial conditions produce similar results to the example presented here.

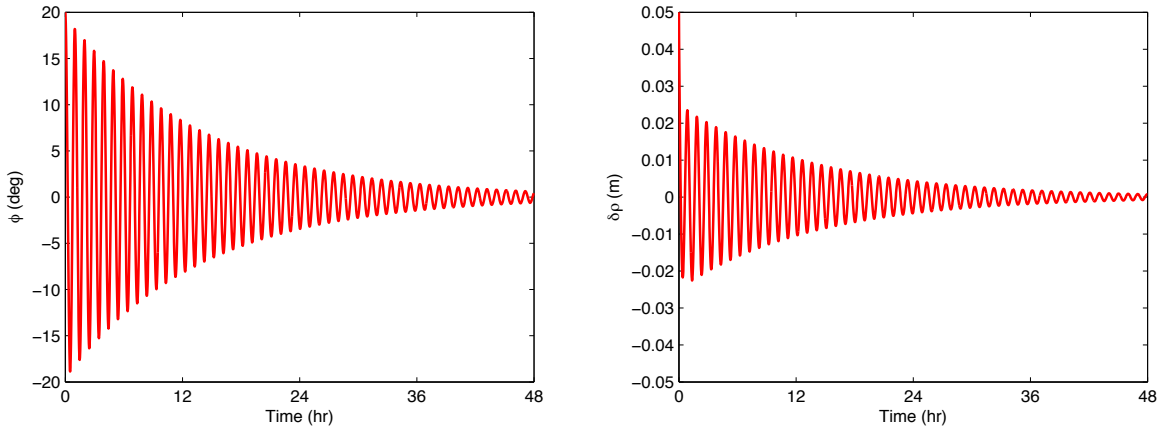

Figure 7. Linear response to a 20° initial libration angle. On the left is the libration angle while on the right is the axial distance between nanosatellites. Over two days, the libration amplitude decays from 40° to under 2°.

D. Nonlinear Response

The linear response was successfully verified against the nonlinear response for a variety of initial conditions. Librational damping performance was found to be robust to variations in initial conditions. One case is presented here for discussion. The initial conditions used are:

$$\phi(0) = 80^\circ \qquad \dot{\phi}(0) = 0 \tag{28}$$

$$\rho(0) = 0.05 \text{ m} \qquad \dot{\rho}(0) = 0.001 \text{ m/s}. \tag{29}$$

The initial separation represents a typical distance between two nanosatellites packaged together. The small value for $\dot{\rho}_0$ represents a nudge between the two satellites upon deployment. The initial libration angle of 80° orients the system nearly horizontally. A more vertical initial condition typically results in faster settling. The initial rotation rate is set to zero.

Figures 8 and 9 depict the motion of the two satellites after separation. The simulation results shown here are typical of other initial conditions. In cases where the system is initially in a higher energy state, the two satellites can spin about each other several times once the tether becomes taut. Axial damping, however, removes enough energy stopping the rotations after about five revolutions.

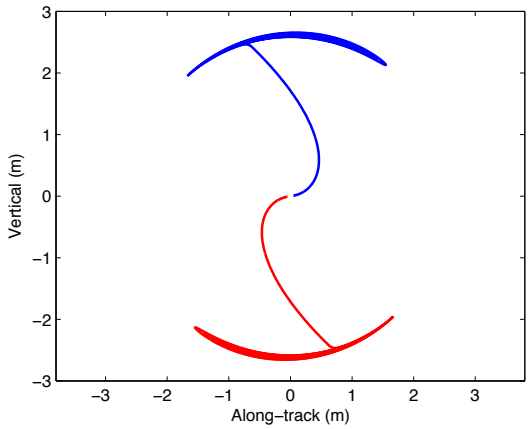

Figure 8. The trajectories of the two nanosatellites are plotted in the local level frame starting at deployment. At first they are close together at $2\rho(0) = 10$ cm. They then drift apart slowly. Once the tether reaches its free limit, they start librating and oscillating in the axial direction. Both types of oscillations damp out.

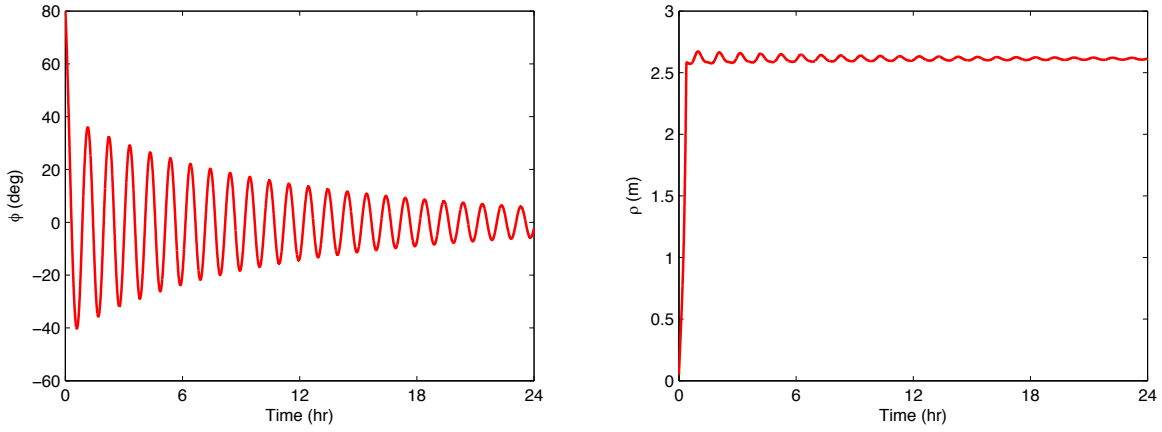

Figure 9. Time-histories are plotted of the satellite libration angle (left) and axial half-distance (right). Librations clearly decay over the 24-hour period shown.

V. Energy Analysis

The total specific energy of the tethered nanosatellite system is

$$e = \left\{ \frac{1}{2}\left(\dot{r}^2 + (r\dot{\theta})^2\right) - \frac{\mu}{r} \right\} + \frac{1}{2}\left\{\rho(\dot{\theta}+\dot{\phi})\right\}^2 - \frac{\mu}{r}\left\{ \left(\frac{\rho}{r}\right)^2 \frac{3\cos^2\phi - 1}{2} \right\} + \left\{ \frac{1}{2}\dot{\rho}^2 + \frac{k}{2m}\left(\rho - \frac{\ell}{2}\right)_+^2 \right\} \quad (30)$$

where $(\cdot)_+$ is equal to the enclosed expression when the tether is taut ($\rho \geq \frac{\ell}{2}$) and equal to zero when slack. The right-hand side of this equation is grouped into the following four terms, ordered as they are in the equation:

1. Orbital energy (kinetic and potential);
2. Librational kinetic energy;
3. Local gravitational potential energy (variation due to librations);
4. Axial energy (linear kinetic and spring potential).

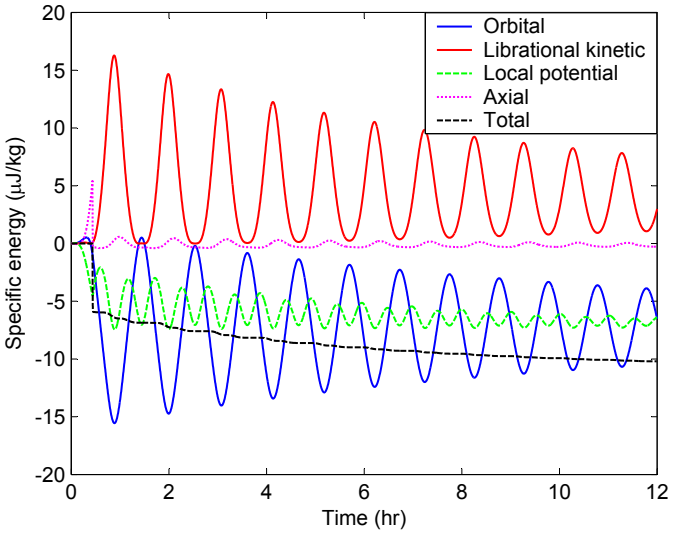

Figure 10. The two curves with large oscillations at the 58-minute libration period are librational kinetic energy (upper) and orbital energy (lower). As the system librates, the primary exchange mechanism is between these two energies. The curves with much smaller oscillations are axial energy (upper) and local potential energy (lower). The declining curve with no oscillations is the total energy, being drawn down as the librations and axial vibrations damp out. All quantities are plotted relative to their initial values.

Figure 10 shows the exchange of energies for the nonlinear case presented in the last section. Several observations are made:

- The total energy is decreasing as the librations and axial vibrations damp out. The local potential energy is drawn down with total energy almost in unison, but with prominent librational oscillations.
- The dominant energy exchange is between librational and orbital energy, *not* between librational kinetic and local potential energy as it would be for a simple pendulum. Librational energy leaks into the orbital dynamics, resulting in the exchange.
- Even though the center of mass is placed in a circular osculating orbit, the librating system induces energy exchange between orbital kinetic and orbital potential (not shown in Fig. 10). This phenomenon is easier explained on the basis of angular momentum, which must be conserved by slighty varying the orbit of the center of mass. With regard to energy, the resulting orbital deviation is important for balancing energy properly, but in terms of distance, the deviation is miniscule (ranging from μm to mm for small satellite systems).

Lyapunov stability analysis can be applied to this problem. It can be shown that the total specific energy e given in Eq. (30) is a Lyapunov function for the nonlinear system. To help see this, the specific dissipation power of the spring-damper mechanism is

$$p = \left\{ \frac{b}{m} \dot{\rho}^2 \right\}_+ \tag{31}$$

where $\{\cdot\}_+$ is given above. The specific dissipation power p is positive semidefinite and satisfies $\dot{e} = -p$ which makes the total specific energy e given in Eq. (30) a Lyapunov function if e can be shown to be positive definite. We have shown by simulation that e is positive definite over a large portion of its nonlinear phase space. Except for initial conditions that start motionless exactly on the unstable equilibrium, or those that terminate at the unstable equilibrium in infinite time, the system as tuned possesses superior transient characteristics. The exceptional initial conditions rarely occur in practice; there is always some imperfection or disturbance that will drive the solution away from the unstable equilibrium, towards the stable equilibrium.

We have investigated the possibility of certifying global stability using this Lyapunov function, but have not yet reached that point. The difficulty lies in the fact that there could be periods of time when the tether is slack, when there is no dissipation of energy at all. But the ever-present centripetal force induced by the gravity gradient tends to force the two nanosatellites apart, the tether favoring tautness over slackness. In nearly all our simulations, the tether became taut quickly (an hour) and stayed taut, thus we believe a case can be made for global stability.

VI. Conclusion

A method for the gravity-gradient stabilization of an orbiting pair of nanosatellites tethered together was investigated where motion is restricted to the orbital plane. A simple passive spring-damper mechanism is placed along the length of the tether which, when tuned properly, damps out both in-plane librational motion and axial vibrations. Using this method, librational amplitude is reduced to about 5° within a day after deployment and less than 1° within two days. The method relies on tuning the spring and damping constants to frequency match the librational dynamics with the axial dynamics. To do this, the spring constant must be small (non-stiff) and the damping constant must be tuned to match the spring constant. Librational energy, normally difficult and slow to dissipate, is then maximally transferred to axial motion where it is easily dissipated. Except when near the unstable equilibrium, initial conditions over a large region of the phase space result in favorable transient performance. Furthermore, the design is robust with respect to the damping constant: variations in its value by an order of magnitude higher or lower do not significantly degrade transient performance.

Possible extensions to this work include:

- Selecting appropriate tether material and spring-damper mechanisms.
- Investigating deployment strategies: how to set up the appropriate initial conditions.
- Consideration of tangling properties of the tethered system.
- The method does not stabilize out-of-plane librations. An alternate approach was considered early on in the investigation: use rotational spring-dampers offset from the center of mass of each nanosatellite. Will this approach perform better? Will it stabilize out-of-plane librations?
- Investigate the effect of continuous disturbances by covariance analysis. Disturbance models would be needed for force or torque disturbances such as solar radiation pressure, atmospheric and magnetic drag, and gravitational attraction of other celestial bodies.

Appendix

The following relationships are useful when simulating the motion of the tethered nanosatellite system. When substituted into the equations of motion that appear in the the main text, the equations of motion are then expressed entirely in terms of the eight phase variables: u, v, ρ, ϕ, $\dot{u}$, $\dot{v}$, $\dot{\rho}$ and $\dot{\phi}$.

Referring to Fig. 1, the polar description of the system center of mass is

$$r = \sqrt{u^2 + (v + r_0)^2} \tag{32}$$

$$\cos(\theta - \theta_0) = \frac{v + r_0}{r} \tag{33}$$

$$\sin(\theta - \theta_0) = \frac{u}{r}. \tag{34}$$

From elementary dynamics, $\dot{r}$ and $\dot{\theta}$ follow from

$$\begin{bmatrix} \dot{r} \\ r\dot{\theta} \end{bmatrix} = \begin{bmatrix} \cos(\theta - \theta_0) & \sin(\theta - \theta_0) \\ -\sin(\theta - \theta_0) & \cos(\theta - \theta_0) \end{bmatrix} \begin{bmatrix} \dot{v} - \omega_0 u \\ \dot{u} + \omega_0(v + r_0) \end{bmatrix} \tag{35}$$

while $\ddot{r}$ and $\ddot{\theta}$ can be found from

$$\begin{bmatrix} \ddot{r} - r\dot{\theta}^2 \\ r\ddot{\theta} + 2\dot{r}\dot{\theta} \end{bmatrix} = \begin{bmatrix} \cos(\theta - \theta_0) & \sin(\theta - \theta_0) \\ -\sin(\theta - \theta_0) & \cos(\theta - \theta_0) \end{bmatrix} \begin{bmatrix} f_v \\ f_u \end{bmatrix} \tag{36}$$

where f_u and f_v appear in Eqs. (3) and (4) of the main text.

Acknowledgments

We acknowledge the U.S. National Science Foundation (NSF) and the Canadian Natural Sciences and Engineering Research Council (NSERC) for providing graduate research fellowships which helped make this work possible.

References

[1]Bentley, D. P. and Tisdale, D., "Development testing of TSS-1 Deployer tether control system mechanisms," *3rd International Conference on Tethers in Space - Toward Flight*, American Institute of Aeronautics and Astronautics, San Francisco, CA, May 17–19 1989, pp. 352–360.

[2]Barnds, W. J., Coffey, S. L., and Davis, M. A., "Determination of TiPS libration using laser radar," *Laser Radar Technology and Applications III*, edited by G. W. Kamerman, Vol. 3380 of *Society of Photo-Optical Instrumentation Engineers (SPIE) Conference*, 1998, pp. 231–242.

[3]Wikipedia, The Free Encyclopedia, *Multi-Application Survivable Tether*, 2007.

[4]Kershner, R. B., "Gravity-Gradient Stabilization of Satellites," *Astronautics and Aerospace Engineering*, September 1963, pp. 18–22.

[5]Carroll, J. A., "Guidebook for Analysis of Tether Applications," Final Report on Contract RH4-394049, Martin Marietta Corporation, March 1985.

[6]Watanabe, Y. and Nakamura, Y., "Orbit Control for a Spacecraft via the Gravity Gradient Force," *IAF-98-A.2.08*, International Astronautical Federation, 1998.